

# Experimental Evaluation of 3D Heat Flow Using Magneto-Thermoelectric Effects in a Ferromagnetic Nanowire

Md Kamruzzaman, Shaojie Hu, Kohei Ohnishi, and Takashi Kimura\*

Herein, a systematic measurement of magneto-thermoelectric voltage induced in a ferromagnetic permalloy nanowire under the operation of a laterally configured nanospintronic device is performed. It is shown that the angular dependences of the magneto-thermoelectric signals with various probe configurations can be quantitatively understood by the combination of the magneto-Seebeck and anomalous Nernst effects. Surprisingly, the contribution of the transverse magneto-Seebeck effect becomes significant in a certain probe configuration, indicating the importance of the transverse heat flow. These results allow us to analyze the 3D distribution of the heat flow inside the permalloy nanowire. The present demonstration indicates that the magneto-thermoelectric effect is a powerful and reliable tool for analyzing the heat distribution in nanostructured devices.

On the other hand, there has been growing interest in energy conversion from the heat and management of the heat flow using spin-dependent phenomena. This is known as spin caloritronics, which is the branch field of spintronics and could provide new opportunities to expand the functionality over conventional electron-based thermoelectric effects.<sup>[9–15]</sup> In addition, renewed interest in magneto-thermoelectric effects has been attracted with the developments of spintronics and spin caloritronics. Especially, recent nanofabrication techniques enable us to prepare an appropriate platform for investigating the thermoelectric effects. However, it is still a serious milestone to develop the reliable method

## 1. Introduction

In highly integrated functional electronic devices with the lateral dimension down to nanometer scale, the power dissipation is one of the most serious obstacles owing to the significant Joule heating effect.<sup>[1–3]</sup> Understanding heat transport in nanoscale devices is a key for designing energy-efficient circuits as well as for energy harvesting systems. As the computational analysis of the heat transport in such nanosized regime, where the mean free path and phase coherent length are comparable to the device dimension, remains uncertainty, the development of the experimental characterization for the heat distribution is indispensable.<sup>[4]</sup> Thermal imaging technique based on the infrared radiation is attractive mean for visually understanding the temperature distribution of the surface of the electric devices.<sup>[5–8]</sup> However, the high reflection from the metallic electrodes significantly prevents the precise analysis using the conventional techniques. In addition, the limited spatial resolution is a serious issue for analyzing the nanoelectric devices.


for analyzing the thermoelectric phenomena in nanosized devices. Here, we carefully and systematically performed the experiments on the magnetic field dependence of the thermoelectric effects in laterally configured ferromagnetic/nonmagnetic hybrid nanostructured devices. We show that the 3D temperature distribution can be analyzed by the combination of the spin-dependent and magneto-thermoelectric effects.

We have fabricated a laterally configured ferromagnetic/nonmagnetic hybrid structure, consisting of a ferromagnetic permalloy (Py) wire and a Pt wire bridged by a Cu strip. Here, the Py is composed of 80% Ni and 20% Fe. **Figure 1** shows a scanning electron microscope image of the fabricated device together with its schematic illustration. The device has been fabricated on a Si substrate whose surface was thermally oxidized for the formation of 1  $\mu\text{m}$ -thick  $\text{SiO}_2$ . The thicknesses for the Py wire, Pt wire, and the Cu strip are 10, 10, and 100 nm, respectively. Prior to the Cu deposition, the surfaces for the Py and Pt wires were well cleaned by the low-voltage Ar ion milling. The electrical resistivities for Py, Pt, and Cu are 33.9, 21.8, and 2.98  $\mu\Omega\text{ cm}$  at room temperature, respectively. In the present device, the Pt wire was used as an electrical heater. The generated heat propagates through the Cu strip as well as the substrate. As the temperature change due to the Joule heating is proportional to the current square, we can effectively pick up the thermoelectric voltage by using the second harmonic detection technique based on the Seebeck effect.<sup>[16–18]</sup>

Before the evaluation of the magneto-thermoelectric effects, we first measured the anisotropic magnetoresistance (AMR) of the Py nanowire for various direction of the magnetic field. Here, we measure the standard first harmonic lock-in technique with a low excitation current whose magnitude of 1  $\mu\text{A}$  with the measurement configuration is shown in **Figure 2a**. The purpose of this experiment is to evaluate the electrical property for the Py

M. Kamruzzaman, S. Hu, K. Ohnishi, T. Kimura  
Department of Physics  
Kyushu University  
744 Motoooka, Fukuoka 819-0395, Japan  
E-mail: t-kimu@phys.kyushu-u.ac.jp

M. Kamruzzaman  
Department of Physics  
University of Dhaka  
Dhaka 1000, Bangladesh

 The ORCID identification number(s) for the author(s) of this article can be found under <https://doi.org/10.1002/pssr.202100608>.

DOI: 10.1002/pssr.202100608

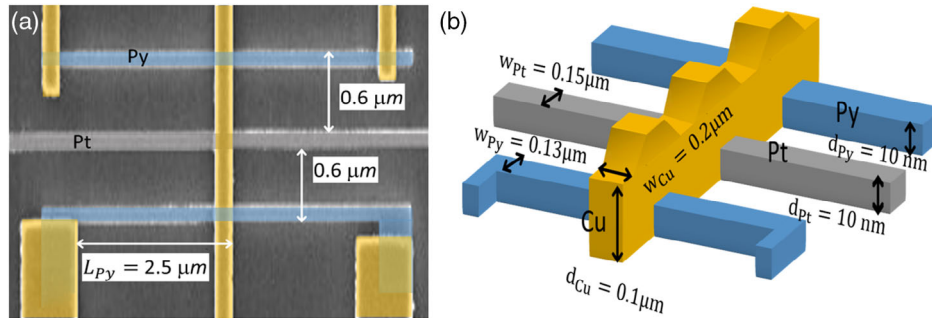


**Figure 1.** a) Scanning electron microscope (SEM) image of the fabricated lateral structure consisting of two Py wires bridged by a Cu strip and b) its schematic illustration with the device geometries.

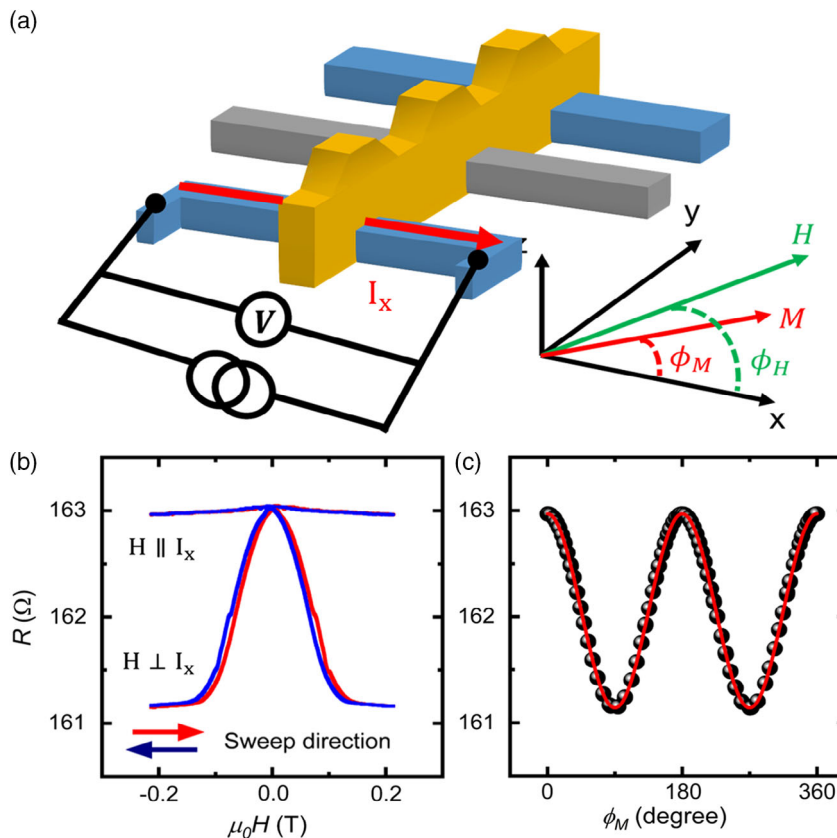


**Figure 2.** a) Schematic illustration of the measurement probe configurations and coordinate systems for AMR measurement. b) Longitudinal and transverse MR curves. The magnetic field is swept up to  $\pm 0.2$  T. The red and blue curves correspond to the forward and backward field sweeps, respectively. c) Angular dependence of the MR change under the magnetic field of 0.2 T for  $\phi_M$ . The solid red lines are corresponding to the fitted curves.

wire and to precisely estimate the direction of the magnetization under the in-plane magnetic field. As can be seen in Figure 2c, the ratio of resistance change due to the magnetization rotation normalized by the base resistance is 1.1%, which is a typical AMR ratio for the permalloy films. This assures the quality of the present Py nanowire. It should be noted that when the magnetic field is not parallel to the easy axis, the direction of the magnetization  $\phi_M$  is not fully aligned with the direction of the magnetic field  $\phi_H$  because of the large shape anisotropy of the magnetic wire. By assuming the  $\cos^2 \phi_M$  angular dependence

of the magnetoresistance change due to AMR,  $\phi_M$  can be simply estimated as a function of  $\phi_H$ . Although this problem can be solved by increasing the magnitude of the external magnetic field, the application of the strong magnetic field may induce other extra effects such as the Lorentz and Hanle magnetoresistances.<sup>[19–22]</sup> In addition, in realistic situations for characterizing the temperature distribution of the practical device, it is difficult to realize to apply the strong magnetic field. Therefore, it is indispensable to develop the characterizing method without using a strong magnetic field.

We then evaluate the thermoelectric effect in the Py wire under the transverse magnetic field. According to our previous study, in order to induce the efficient Seebeck voltage, the ferromagnetic voltage probe should be located to the far side from the Pt heater. This is because the heat flow through the substrate plays a significant role for inducing the efficient temperature difference between the voltage terminals  $V_+$  and  $V_-$ . **Figure 3b** shows the second harmonic voltage for various bias currents. The AMR-like field dependence with the opposite sign is clearly confirmed by increasing the bias current, indicating the clear observation of the anisotropic magneto-Seebeck (AMS) effect. It also should be noted that a small asymmetry is observed with respect to the reversal of the external magnetic field along  $y$  axis. This is the unique signature of the second harmonic voltage

In order to analyze the second harmonic voltage more quantitatively, we have defined the background voltage  $V_B$ , symmetric voltage change  $V_S$ , and asymmetric voltage change  $V_{AS}$  as follows.  $V_B = V_1$ ,  $V_S = (V_2 + V_3 - 2V_1)/2$ , and  $V_{AS} = (V_2 - V_3)$ , where  $V_1$ ,  $V_2$ , and  $V_3$  are the voltage at  $H = 0$ , that at  $H = +0.2$  T and that at  $-0.2$  T, respectively. **Figure 3b,c** show the bias current dependencies of  $V_B$ ,  $V_S$ , and  $V_{AS}$ . Parabolic dependencies can be clearly seen, indicating the definite evidence of the thermal nature of the second harmonic signals,  $V_B$ ,  $V_S$ , and  $V_{AS}$ . The induced voltage due to the Seebeck effect is given by  $(S_{Py} - S_{Cu})\Delta T$ , where  $\Delta T$  is the temperature difference between the junction for the Py wire and the  $V_+$  Cu probe and that for the Py wire and the  $V_-$  Cu probe. The symmetric field dependence of the second harmonic voltage is caused by the anisotropy of the Seebeck coefficient for the Py wire.<sup>[23,24]</sup> Here, we estimate the AMS ratio, which is defined by  $(S_{Py}^\perp - S_{Py}^\parallel)/S_{Py}^\parallel$ , where  $S_{Py}^\perp$  and

$S_{Py}^\parallel$  are, respectively, the Seebeck coefficient for the case of the heat current parallel to the magnetization and that of the heat current perpendicular to the magnetization. According to the previous studies,  $S_{Py}^\parallel$  and  $S_{Cu}$  are given by  $-18.0$  and  $1.6 \mu V K^{-1}$ , respectively.<sup>[25]</sup> Using the relative relationship  $S_{Py}^\parallel/S_{Cu} = -11.25$ , we obtain  $S_{Py}^\parallel \Delta T$  as  $50.5 \mu V$ . As  $\Delta V^{2\omega}$  is given by  $(S_{Py}^\perp - S_{Py}^\parallel)\Delta T$ , the AMS ratio for the Py can be estimated as 0.6%, which is approximately a half value of the AMR ratio. Although the estimated value is consistent with the previous study, this small AMS change makes it difficult to analyze the magneto-thermoelectric effect in magnetic nanostructures precisely.

As  $V_{AS}$  is also confirmed to be the thermal nature, we should take into account the anomalous Nernst effect (ANE), which is another representative magneto-thermoelectric effect in ferromagnetic metals.<sup>[16]</sup> To confirm that the origin of the asymmetric field dependence of the thermoelectric voltage is related to the ANE, we measure the angular dependence of the second harmonic voltage at  $H = 0.2$  T. According to the ANE, the transverse electric voltage along  $x$  axis can be induced by the heat current along  $z$  direction in association with the magnetization of  $y$  component. Here, the heat current along the  $z$  direction can be understood by the heat diffusion into the substrate. Therefore, the ANE voltage should show  $\sin \phi_M$  dependence. **Figure 3e** shows the angular dependence of the second harmonic voltage. Although the angular dependence mainly shows  $-\cos 2\phi_M$  dependence originating from the AMS, a small  $\sin \phi_M$  dependence can be confirmed. In order to analyze the experimental results more quantitatively, we fit the obtained curve by using the following equation.

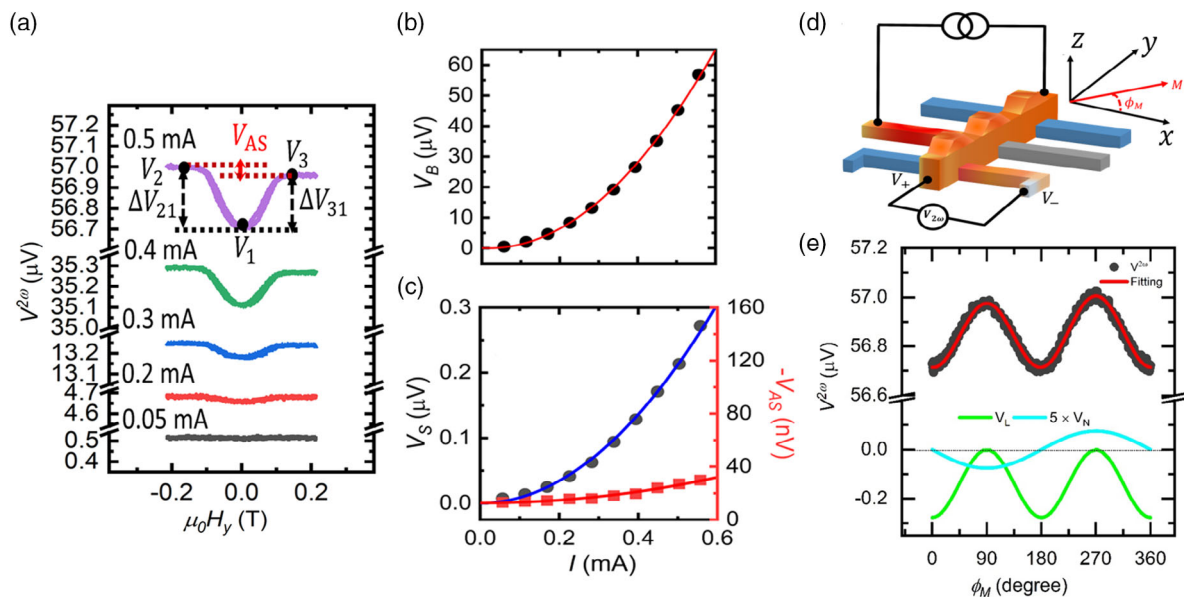


**Figure 3.** a) Transverse field ( $H_y$ ) dependence of the second harmonic voltages for the various AC bias currents under the Joule heating of the Pt wire. Bias current dependence of b) the background voltage  $V_B = (V_1 + V_2 + V_3)/3$ , c) the symmetric voltage  $V_S = (V_2 + V_3 - 2V_1)/2$ , and the asymmetric field dependence of the second harmonic voltage  $V_{AS} = (V_2 - V_3)$ , together with the solid line of the parabolic fitted curves. d) Schematic illustration of the measurement configuration for the anisotropic magneto-Seebeck effect. e) Angular dependence of the second harmonic voltage under the magnetic field of 0.2 T. The black solid dots curves are the experimental data. The solid red lines correspond to the fitted curves using Equation (1). The green and cyan lines correspond to the thermospin voltage of  $V_{AMS}$  and  $V_{ANE}$ , respectively.

$$V_{2\omega}(\phi_M) = V_0 + \Delta V_{\text{AMS}} \cos 2\phi_M + \Delta V_{\text{ANE}} \sin \phi_M \quad (1)$$

Here,  $V_0$  is the background voltage;  $\Delta V_{\text{AMS}}$  and  $\Delta V_{\text{ANE}}$  are the voltage change due to the AMS and that due to the ANE. The fitting curve with  $V_0 = 56.85 \mu\text{V}$ ,  $\Delta V_{\text{AMS}} = 0.14 \mu\text{V}$ , and  $\Delta V_{\text{ANE}} = -0.018 \mu\text{V}$  well reproduces the experimental angular dependence, assuring that  $V_{\text{AS}}$  is caused by the ANE.

To obtain more definite evidence, we have performed the similar systematic measurements with the different probe configuration, where  $V_+$  terminal is located to the near side of the Pt heater, as shown in **Figure 4a**. According to our previous study, in this probe configuration, owing to the significant heat flow from the substrate the temperature difference  $\Delta T$  dramatically decreases. As a result, the second harmonic voltage due to the Seebeck effect is reduced. On the other hand, owing to the increase of the heat flow through the substrate, the enhancement of  $V_{\text{AS}}$  due to the ANE is expected. **Figure 4b** shows the second harmonic signal using the near-side  $V_+$  voltage probe as a function of the magnetic field along  $\gamma$  direction. Although the reduction of the background voltage is clearly observed, the field dependence of the second harmonic voltage shows a dramatically different feature. In addition, the magnitude of  $V_{\text{asy}}$  does not increase so much and reverses the sign. This implies that the heat current along  $z$  axis in the near-side Py wire is reversed from that in the far-side Py wire.

First, we consider the sign change of the  $V_{\text{AS}}$  between two configurations. In the far-side Py wire, the heat mainly comes from the Cu wire. Therefore, the heat in the Py wire propagates along the wire ( $x$  direction) with the diffusion into the substrate. As a result, the heat current along the  $z$  axis becomes negative in a far-side Py wire. On the other hand, in the near-side Py wire, the heat flow from the substrate overcomes the heat flow from the Cu wire, resulting in the positive heat current along  $z$  axis. Thus, the sign change of  $V_{\text{AS}}$  without a significant increase of the magnitude can be understood by the sign reversal of the heat current for  $z$  component.

We then discuss about the unconventional field dependence of the second harmonic voltage. In order to find out the mechanism of the unexpected field dependence, we have measured the

angular dependence of the second harmonic voltage at  $H = 0.2 \text{ T}$ .

As can be seen in **Figure 4c**, the angular dependence of  $V_{2\omega}$  seems to show  $\sin 2\phi_M$  with a small deviation. Here, a small deviation should be caused by the AMS and ANE. To analyze the result more quantitatively, we fit the curve by using the following modified equation with taking into account the unknown term given by  $\Delta V_{\text{un}} \sin 2\phi_M$ .

$$V_{2\omega}(\phi_M) = V_0 + \Delta V_{\text{AMS}} \cos 2\phi_M + \Delta V_{\text{ANE}} \sin \phi_M + \Delta V_{\text{un}} \sin 2\phi_M \quad (2)$$

The fitting curve with  $V_0 = -15.15 \mu\text{V}$ ,  $\Delta V_{\text{AMS}} = 0.06 \mu\text{V}$ ,  $\Delta V_{\text{ANE}} = 0.03 \mu\text{V}$ , and  $\Delta V_{\text{un}} = 0.32 \mu\text{V}$  well reproduces the experimental angular dependence. Thus,  $\sin 2\phi_M$  dependence is a dominant contribution of the second harmonic voltage with the probe configuration using the near-side Py voltage terminal.

As the origin of  $\sin 2\phi_M$  dependence, we consider the influence of the heat current along  $\gamma$  axis. This is because the AMS and ANE are caused by the heat flow along the  $x$  axis and that along  $z$  axis, respectively. Similarly, in the AMR and planar Hall effect in the electrical measurements, the magnetization induces not only the longitudinal Seebeck voltage but also the transverse one with respect to the direction of the heat flow. This transverse Seebeck effect could contribute to the main field dependence in the second harmonic voltage in the near-side Py wire, namely, transverse magneto-Seebeck effect or planar Nernst effect.<sup>[26,27]</sup> Similarly, in the electrical magnetoresistance measurement, the transverse magneto-Seebeck voltage provides the consistent description for  $\sin 2\phi_M$  dependence in the second harmonic voltage. We emphasize that the amplitude of the transverse Seebeck effect is approximately two times larger than the longitudinal Seebeck effect in the cross configuration. This means that the heat current along the  $\gamma$  axis is effective for the efficient generation of the thermoelectric voltage.

To obtain more definite evidence, we also performed the similar experiment by using another ferromagnetic wire located in the opposite side of the Pt heater. In this configuration, the heat current along the  $\gamma$  direction is reversed from the previous

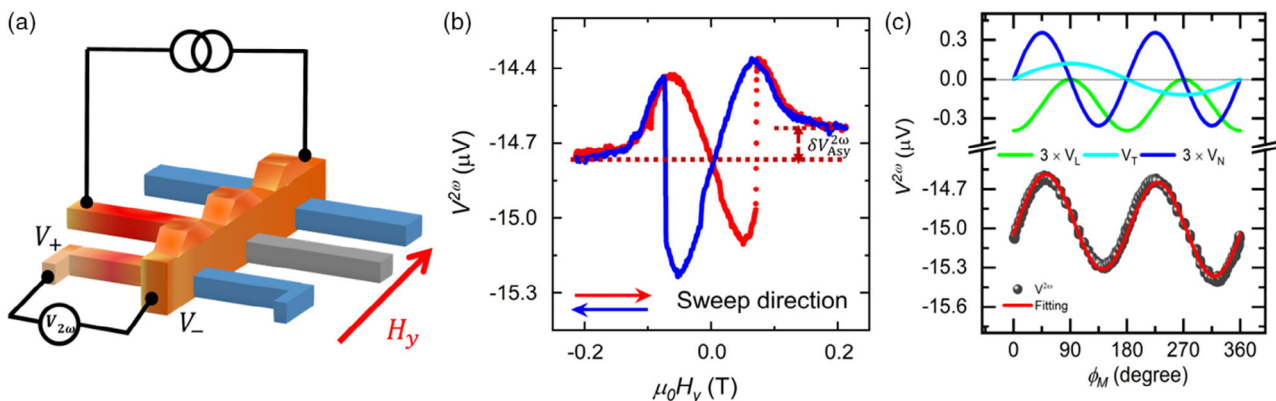


**Figure 4.** a) Schematic presentation of the measurement configuration using the near-side ferromagnetic voltage probe. b) Transverse field ( $H_y$ ) dependence of the second harmonic voltage. The forward and backward field sweep is represented by red and blue curves. c) Angular dependence of the second harmonic voltage under the magnetic field of 0.2 T. The solid red lines correspond to the fitted curves using Equation (2). The green, blue, and cyan lines correspond to the three thermospin voltage of  $V_{\text{AMS}}$ ,  $V_{\text{un}}$ , and  $V_{\text{ANE}}$ , respectively.



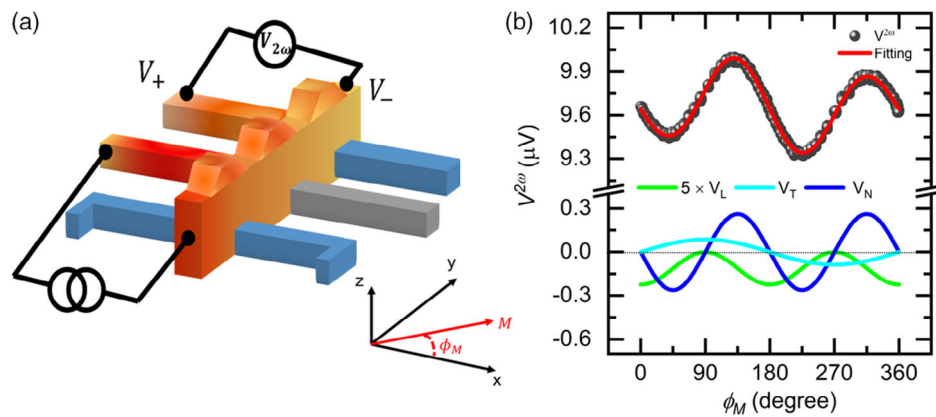


**Figure 5.** a) Measurement configuration for the magneto-thermoelectric effects using another Py wire. b) Angular dependence of the second harmonic voltage under the magnetic field of 0.2 T. The solid red lines correspond to the fitted curves using Equation (2). The green, blue, and cyan lines represent  $V_{AMS}$ ,  $V_{un}$ , and  $V_{ANE}$ , respectively.

configuration while those for  $x$  and  $z$  axes are maintained with the same direction. **Figure 5b** shows the angular dependence of the second harmonic voltage with the probe configuration shown in **Figure 5a**. As we expected, the result is well reproduced by the fitting curve with the opposite sign for  $\Delta V_{un}$ . Thus, the output thermoelectric voltage is understood by the combination of longitudinal and transverse Seebeck and ANE. We emphasize that a small temperature change along  $y$  direction produces the significant thermoelectric voltage. This kind of the thermoelectric voltage due to the undesired heat flow should be taking into account in variety of spintronic devices especially in a heavy metal/ferromagnet bilayer, which is a typical device structure using spin Hall effect.<sup>[28,29]</sup>

In summary, we have systemically investigated the magneto-thermoelectric effects in the Py nanowire under the various direction of the in-plane magnetic field. The second harmonic voltage detection enables us to observe a clear AMS effect whose magnitude is two times smaller than the electrical AMR. From the systematic probe configuration dependence with its the angular dependence, the magneto-thermoelectric voltage is found to be caused by not only the longitudinal heat current but also the transverse heat current. Especially, in a certain probe configuration, the voltage change due to the planar Nernst effect becomes a much larger than that for the AMS, indicating the possibility for the efficient generation of the thermoelectric voltage. Our demonstration will pave the way to develop nanoheat sensors using the magneto-thermoelectric effect in ferromagnetic metal nanowires.

## Acknowledgements

This work was partially supported by Grant-in-Aid for Challenging Research (Pioneering) (grant no. 17H06227) and JST CREST (grant no. JPM1CR18J1).

## Conflict of Interest

The authors declare no conflict of interest.

## Data Availability Statement

The data that support the findings of this study are available from the corresponding author upon reasonable request.

## Keywords

anomalous Nernst effect, magneto-Seebeck effect, spintronic devices

Received: December 6, 2021

Revised: January 12, 2022

Published online:

- [1] E. Pop, *Nano Res.* **2010**, *3*, 147.
- [2] N. Yang, X. Xu, G. Zhang, B. Li, *AIP Adv.* **2012**, *2*, 041410.
- [3] D. G. Cahill, P. V. Braun, G. Chen, D. R. Clarke, S. Fan, K. E. Goodson, P. Keblinski, W. P. King, G. D. Mahan, A. Majumdar, H. J. Maris, S. R. Phillpot, E. Pop, L. Shi, *Appl. Phys. Rev.* **1**, 2014.
- [4] P. Keblinski, S. R. Phillpot, S. U. S. Choi, J. A. Eastman, *Int. J. Heat Mass Transfer* **2002**, *45*, 855.
- [5] B. R. Gopal, R. Chahine, M. Földeäki, T. K. Bose, *Rev. Sci. Instrum.* **1995**, *66*, 232.
- [6] H. Straube, J.-M. Wagner, O. Breitenstein, *Appl. Phys. Lett.* **2009**, *95*, 052107.
- [7] J. Döntgen, J. Rudolph, T. Gottschall, O. Gutfleisch, S. Salomon, A. Ludwig, D. Hägele, *Appl. Phys. Lett.* **2015**, *106*, 032408.
- [8] S. Daimon, R. Iguchi, T. Hioki, E. Saitoh, K. Uchida, *Nat. Commun.* **2016**, *7*, 13754.
- [9] I. Žutić, J. Fabian, S. D. Sarma, *Rev. Mod. Phys.* **2004**, *76*, 323.
- [10] G. E. W. Bauer, A. H. MacDonald, S. Maekawa, *Solid State Commun.* **2010**, *150*, 459.
- [11] M. Johnson, *Solid State Commun.* **2010**, *150*, 543.
- [12] G. E. W. Bauer, E. Saitoh, B. J. van Wees, *Nat. Mater.* **2012**, *11*, 391.
- [13] S. R. Boona, R. C. Myers, J. P. Heremans, *Energy Environ. Sci.* **2014**, *7*, 885.
- [14] H. Yu, S. D. Brechet, J. P. Ansermet, *Phys. Lett. Sect. A* **2017**, *381*, 825.
- [15] K. Uchida, *Proc. Jpn. Acad. B* **2021**, *97*, 69.
- [16] S. Hu, T. Kimura, *Phys. Rev. B* **2013**, *87*, 014424.
- [17] S. Hu, H. Itoh, T. Kimura, *NPG Asia Mater.* **2014**, *6*, 127.

- [18] S. Hu, T. Nomura, G. Uematsu, N. Asam, T. Kimura, *Phys. Rev. B* **2016**, *94*, 014416.
- [19] R. P. Van Gorkom, J. Caro, T. M. Klapwijk, S. Radelaar, *Phys. Rev. B* **2001**, *63*, 134432.
- [20] I. Knittel, U. Hartmann, *J. Magn. Magn. Mater.* **2005**, *294*, 16.
- [21] S. Vélez, V. N. Golovach, A. Bedoya-Pinto, M. Isasa, E. Sagasta, M. Abadia, C. Rogero, L. E. Hueso, F. S. Bergeret, F. Casanova, *Phys. Rev. Lett.* **2016**, *116*, 016603.
- [22] H. Wu, X. Zhang, C. H. Wan, B. S. Tao, L. Huang, W. J. Kong, X. F. Han, *Phys. Rev. B* **2016**, *94*, 174407.
- [23] E. Yong Pu, *Phys. Rev. Lett.* **2006**, *97*, 1.
- [24] J. Kimling, J. Gooth, K. Nielsch, *Phys. Rev. B* **2013**, *87*, 094409.
- [25] F. K. Dejene, J. Flipse, B. J. Van Wees, *Phys. Rev. B* **2012**, *86*, 024436.
- [26] A. D. Avery, M. R. Pufall, B. L. Zink, *Phys. Rev. Lett.* **2012**, *109*, 196602.
- [27] A. D. Avery, M. R. Pufall, B. L. Zink, *Phys. Rev. B: Condens. Matter Mater. Phys.* **2012**, *86*, 1.
- [28] H. Nakayama, M. Althammer, Y.-T. Chen, K. Uchida, Y. Kajiwara, D. Kikuchi, T. Ohtani, S. Geprägs, M. Opel, S. Takahashi, R. Gross, G. E. W. Bauer, S. T. B. Goennenwein, E. Saitoh, *Phys. Rev. Lett.* **2013**, *110*, 206601.
- [29] C. Onur Avci, K. Garello, A. Ghosh, M. Gabureac, S. F. Alvarado, P. Gambardella, *Nat. Phys.* **2015**, *11*, 570.